Chemical Physics 481 (2016) 184–190

Contents lists available at ScienceDirect

Chemical Physics

journal homepage: www.elsevier.com/locate/chemphys

Dynamics of charge at water-to-semiconductor interface: Case study of wet [001] anatase TiO_2 nanowire

Shuping Huang [a,d,e], Choumini Balasanthiran [a], Sergei Tretiak [b], James D. Hoefelmeyer [a], Svetlana V. Kilina [c], Dmitri S. Kilin [a,c,*]

[a] Department of Chemistry, University of South Dakota, Vermillion, USA
[b] Center for Integrated Nanotechnologies, Los Alamos National Laboratory, Los Alamos, NM 87545, USA
[c] Department of Chemistry and Biochemistry, NDSU, Fargo, ND 58108, USA
[d] College of Chemistry, Fuzhou University, Fuzhou 350116, China
[e] Department of Chemistry, University of Minnesota, Minneapolis, MN 55455, USA

ARTICLE INFO

Article history:
Available online 4 August 2016

Keywords:
TiO_2 nanowire
Water splitting
Absorption spectrum
Photoluminescence
Nonadiabatic excited state dynamics
Multilevel Redfield theory
Energy-gap law

ABSTRACT

The behavior of water molecules on the surfaces of the TiO_2 nanowire grown in [001] direction has been investigated by combining theoretical calculations and experiments. Calculated UV–visible absorption spectra reproduce the main features of the experimental spectra. Computations predict that a photoexcitation followed by a sequence of relaxation events results in photoluminescence across the gap. TiO_2 nanowires in vacuum and aqueous environment exhibit different dynamics of photo-excited charge carriers. In water, computed relaxation of electrons (holes) is approximately 2 (4) times faster compared with vacuum environment. Faster relaxation of holes vs. electrons and specific spatial localization of holes result to formation of long lived charge transfer excitation with positive charge at the surface of the nanowire. Comparison of relaxation process in TiO_2/water interfaces focusing on different surfaces and nanostructures has potential in identifying structural characteristics of TiO_2 materials important for efficient photo-electrochemical water splitting.

There is an active search of optimal structures providing highest efficiency of photo-activated water splitting half-reactions $2H^+ + 2e^- \overset{cat_1}{\rightarrow} H_2$ and $2H_2O \overset{cat_2}{\rightarrow} 4H^+ + 4e^- + O_2$. An increase of efficiencies of reducing catalyst cat_1 and oxidation catalyst cat_2 are achieved by choice of appropriate material composition and spatial confinement regime. In this Letter, we test the suitability of one-dimensional (1D) metaloxide semiconductors nanostructures for the role of oxidation catalyst cat_2. Understanding the mechanisms of water adsorption at the surface of such nanostructure and photo-induced dynamics of charge carriers (electron and hole) at the interface between water and semiconductor nanostructure is a fundamental step in finding an optimal material for water splitting in a photo-electrochemical cell [1–3].

The adsorption of water on metal oxide surfaces has been attracting great interest for many years due to its applications in catalysis, photochemistry, and electrochemistry [4–6]. Titanium dioxide (TiO_2), which is nontoxic and has low cost with excellent physical and chemical stability, has attracted particular attention [7]. The surface-to-volume ratio of a TiO_2 nanostructure correlate with its crystallographic phase. Specifically, TiO_2 samples dominated by bulk atoms are typically found as the rutile phase due to its thermodynamic stability; however, samples dominated by surface atoms are typically found as the anatase phase due to the favorable surface free energy of the {101} facet [8–11]. Compared with TiO_2 rutile, TiO_2 anatase is more efficient and more widely used in catalysis and photo-electrochemistry [12,13].

Small complexes of *Ti* ions coordinated to hydroxyl and water, for water splitting applications, were recently described [14–17]. There are extensive experimental and theoretical studies on the H_2O adsorption on anatase surfaces [18–22]. In addition to surfaces, 1D nanostructures i.e. nanowires (NWs) and nano-rods (NRs) promise several beneficial features: 1) better spatial separation of charge carriers; 2) easier transport/conducting along NW axis; 3) additional tuning of electronic and optical properties via spatial confinement; 4) high surface-to-volume ratio maximizing interface with the solvent; 5) larger number of surfaces and edges with various structural symmetry acting as reaction activated sites in surface chemistry; 6) easier manufacturing procedure of nanowire growth providing higher quality, defect-free materials due to relaxation of surface strain that allows avoiding lattice

* Corresponding author at: Department of Chemistry and Biochemistry, North Dakota State University, Fargo, ND, USA.
E-mail addresses: Dmitri.Kilin@usd.edu, Dmitri.Kilin@ndsu.edu (D.S. Kilin).

http://dx.doi.org/10.1016/j.chemphys.2016.08.002
0301-0104/

mismatch [23–28]. There are already few theoretical studies of the H_2O adsorption on anatase TiO_2 NWs [29,30]. Theory and computational modelling of finite NRs and periodic models of NWs can provide additional insights in effect of surface and interface characteristics on the electronic structure and radiative and nonradiative electron dynamics in these systems.

The computational modelling of the carrier relaxation in molecules and nanostructures relies on partitioning the total energy between electronic part and nuclear part and allowing for coupling between them, going beyond Born-Oppenheimer approximation [31–34]. Several successful computational strategies for electronic relaxation are proposed [35–44]. Historically, the electronic relaxation in the limit of long time dynamics, low couplings, and multiple electronic states is often addressed by the multilevel Redfield theory [45–53]. There were recent approaches to combine Redfield theory of electron relaxation with on-the-fly coupling of electrons-to-lattice through a molecular dynamics (MD) trajectory in the basis of density functional theory (DFT) [54–62].

The photo-induced electron transfer at the interfaces of a molecule or a water layer, a graphene-layer, a semiconductor quantum dot or perovskite layer with rutile TiO_2 surfaces has been investigated by Prezhdo et al. [63–68] using real-time nonadiabatic MD [69–72]. These works have provided an understanding of the mechanisms of electron transfer, relaxation, and recombination dynamics, and the effect of these processes on the solar cell efficiencies. Batista et al. [40,41] explored the process of electron injection in catechol/TiO_2-anatase nanostructures at the detailed molecular level to gain a fundamental understanding of excited-state electron-injection paths. Meng and Kaxiras [73,74] investigated the electron and hole dynamics of the systems consisting of organic sensitizers and anatase TiO_2 NWs. Mahran et al. has modelled photo-induced hole transfer from TiO_2 NW to caffeic acid adsorbate [75].

In this work we explicitly consider 1D nanostructures of anatase TiO_2 and study the influence of water adsorption on electronic and optical properties of [001] TiO_2 NRs and NWs by combining density matrix formalism and *ab initio* electronic structure calculations (see Supporting information for Methods) and comparing calculations to experiments. The letter is organized as follows. We start with calculating structural properties, binding energy, charge density, and structure reorganization during molecular dynamics (MD). Next, we analyze electronic properties: band-gap scaling, analysis of UV–vis spectra, and normal mode analysis. Finally, we report signatures of electron-phonon interaction on rates of nonradiative electronic transitions, discuss energy-gap law, and explore mechanisms of photo-excited charge carriers dynamics along with comparison of rates for different excitations, followed by computed photoluminescence spectra. Our findings are briefly summarized at the last paragraph.

Powder X-ray diffraction and TEM data of our synthesized NRs are shown in Figs. S1 and 1a. A minimalistic infinite periodic model of about 1 nm diameter NW along [001] direction, with lateral surfaces derived from cutting by the {100} and {101} surfaces, is constructed to model a finite NR grown along [001] direction. Fig. 1b displays the optimized H_2O adsorbed [001] NW (referred as wet NW) from the side view. The cell size is $0.97 \times 2.0 \times 2.0$ nm matching the periodicity in the [001] direction and adding vacuum in [100] and [010] directions to avoid spurious interactions between periodic replicas of the model. Chemical composition of the cell reads $Ti_{25}O_{50} + 20H_2O$. The simulation cell has several ions that maintain inter-atomic distances and coordination numbers of bulk anatase. Based on these structural symmetry one assumes that properties of this minimalistic model correlate to properties of nanowires/nanorods of larger diameter. The surface Ti–O distances are close to the ones in the core of the NW. The ions belonging to the NWs provide similar O–Ti radial distribution function (RDF) as those of bulk anatase, see Fig. S2. Most of the water molecules are molecularly adsorbed; however, two water molecules are dissociated. The dissociation is observed at a "step" intersection of surfaces: {100} and {010}. Signatures of water adsorption are also seen in O–O and O–H RDF, in Fig. S3.

Adsorption of water leads to two effects: partial dissociation of water and partial reorganization of the surface. Specifically, two Ti–O bonds of the NW are broken. The detailed analysis of restructured geometry is given in Fig. 1(d) caption and in Fig. S4.

The average adsorption energy for each H_2O molecule is −0.73 eV, indicating that the adsorption is exothermic. Moreover, our calculated adsorption energy is the same as the calculated adsorption energy of an isolated H_2O molecule on anatase {101} [19]. According to our PBE calculations the partial dissociation of water molecules on [001] TiO_2 NW is 1.02 eV energetically more favorable than the complete dissociation model reported by Iacomino et al. [29].

To further examine the interactions of the H_2O with TiO_2, we next analyze the spatial distribution of the total charge density difference, shown in Fig. S5. After the water adsorption, the electron densities accumulate in the space regions between the NW and water, except for the region between O1 or O3 and H from the dissociated water molecules. The electron densities of surface Ti atoms especially at the crossing of (1 0 0) and (0 1 0) surfaces deplete. Significant charge rearrangements occur in the regions of O1H, O3H, O2H, and O4H groups and its bonded Ti atoms.

In the dynamical simulations, we equilibrate energy in a thermostat at 300 K for 150 fs, followed by *ab initio* molecular dynamics [76]. During the thermalization and molecular dynamics, the structure of the TiO_2/H_2O interface experiences additional changes. Specifically, O1H, O2H, and O3H groups bond with H atoms of neighbouring H_2O to form new H_2O molecules and OH bonds in Fig. S4a. There is one more H_2O molecule dissociated into OH and H. The dissociated H atom is bonded to a bridge $O_{(2c)}$ atom of NW, and the O–H bond distance is 1.15 Å, which longer than the terminal O–H bonds. At 500 fs in the MD simulation (Fig. 3Sb), one more H_2O is dissociated and one broken Ti–O bond is reformed. Another two bridge OH bonds are formed. There are eight hydroxyl groups in each unit cell. One H_2O forms three hydrogen bonds with a bridge OH ($H_2O\cdots H$ distance is 1.49 Å) and two surface $O_{(2c)}$ atoms of NW ($HOH\cdots O$ distance is 1.36 and 2.27 Å, respectively). During the MD, there are no H_3O^+ and $H_5O_2^+$ ions produced.

Table 1 compares the calculated gaps by different functionals with the respective experimental values. For the wet TiO_2 NW, the calculated direct band gap by GGA-PBE is 2.38 eV, which is larger than the calculated one (2.20 eV) for the bare NW [77–79], because partial surface dangling states disappear, in agreement with the Iakomino's result of water completely dissociative adsorption on TiO_2 NWs [29]. The GGA-PBE functional underestimates the band gap due to the electron self-interaction problem, while the Heyd-Scuseria-Ernzerhof (HSE) screened Coulomb hybrid density functional offers a better description of band gaps [80]. The calculated band gaps of TiO_2 bulk, bare and wet [001] NW by the HSE06 functional are 3.49 eV, 3.67 eV, and 3.78 eV respectively, with a gap increment attributed to quantum confinement and dangling state compensation. Total and projected density of states for dry/wet NW by PBE functional is available in Fig. S6 in comparison with DOS computed by HSE06 functional shown in Fig. S7.

Fig. 1c shows the calculated absorption spectra of the wet NW by the HSE06 functional and the experimental spectra of concentrated TiO_2 NR water solution. Calculated UV–visible absorption spectra reproduce the main features of the experimental spectra. The absorption band of our calculated spectra of $d = 1$ nm NW is blue shifted compared with the experimental

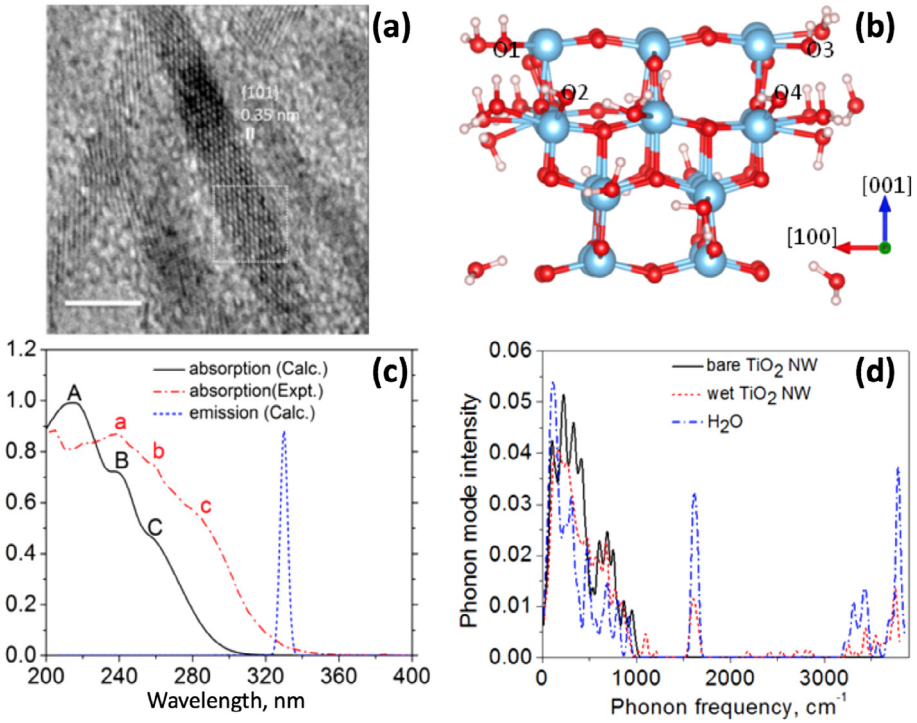

Fig. 1. (a) Transmission electron microscopy of synthesized NRs. The scale bar = 5 nm. (b) Side view of the simulated NW optimized at 0 K. Red, blue, and white spheres stand for O, Ti, and H atoms. (c) The calculated absorption spectrum of wet TiO_2 NW, the experimental spectrum of TiO_2 NR water solution, and the calculated emission spectrum for the excitation at 4.36 eV. (d) The calculated phonon (normal mode) density of states at Γ point for bare TiO_2 NW, wet TiO_2 NW, and H_2O (re-optimization after removing TiO_2 NW) by PBE functional. We label and describe most representative ions in the model: There are four terminal hydroxyl groups (O1H, O2H, O3H, and O4H) formed, of which two oxygen atoms (O1 and O3) are from the NW, and two Ti–O bonds of the NW are broken. The bond distances of Ti–O1, Ti–O2, Ti–O3, and Ti–O4 are 2.00, 1.96, 2.00, and 1.89 Å, respectively. Fifteen H_2O molecules are weakly bonded to 4-coordinated $Ti_{(4c)}$ or 5-coordinated $Ti_{(5c)}$, the Ti–O distances of which are 2.20–2.47 Å. Three H_2O molecules are adsorbed with H atoms pointing toward the 2-coordinated oxygen $O_{(2c)}$ atoms of NW, representing {1 0 1} surface. There are hydrogen bonds formed between neighbour H_2O molecules or adjacent OH group and H_2O molecules. (For interpretation of the references to color in this figure legend, the reader is referred to the web version of this article.)

Table 1
The calculated gaps of [0 0 1] anatase NW by PBE and HSE06 functionals compared to experimental gaps. Notably, reference [78], reports larger PBE gap of 2.69 eV* and HSE06 gap of 4.06 eV**, for a d ~0.75 nm diameter anatase NW in vacuum attributed to stronger quantum confinement.

	Computed direct band-gap E_g, eV		
TiO_2 structure	PBE	HSE	Experiment
Bulk anatase	1.91	3.49	3.20
[0 0 1] nanowire in vacuum	2.20*	3.67**	
[0 0 1] nanowire in water	2.38	3.78	

spectra of d = 3–4 nm NR, which is due to the quantum confinement effect. Each of the feature peaks, *A*, *B*, and *C* in the spectra is attributed to a pair of orbitals indicated in Fig. S7b and plotted in Fig. S8, which give the maximal contribution to the feature (Table S1), while frontier orbitals for lowest excitation are provided in Fig. S9, for comparison. The corrected absorption spectrum using an energy shift parameter from PBE calculations can reproduce the HSE result (Fig. S10a). The corrected emission spectrum for the excitation at 4.36 eV shows a sharp peak at 330 nm.

The comparison of the calculated absorption spectra of bare and wet TiO_2 NWs (Fig. S10b) shows that the adsorption of H_2O on the surface of NW doubles the absorption intensity and the numbers of the peaks of NW decreases compared to the bulk, in agreement with the results for silicon NWs [81]. According to Fig. S7, density of states (DOS) of bare NW shows a sub-gap in the vicinity of −5.5 eV, while wet NW shows a continuous DOS near the valence band maximum. This sub-gap feature can delay hole relaxation in bare NW and the absence of such sub-gap in the wet NW can be responsible for enhancement of hole relaxation in wet NWs.

Fig. 1d shows the calculated phonon density of states of bare TiO_2 NW, wet TiO_2 NW, and remaining water molecules by removing TiO_2 NW computed by the PBE functional. The water molecules, which are optimized after removing TiO_2 NW, form a network with each molecule interacting with about 4 close neighbours, resembling the shape of nanotube. The strong peaks below 1000 cm^{-1} are due to the O–Ti vibration modes and librational (restricted rotational) motions of water molecules. The peaks between 1000 and 1250 cm^{-1} and 1500 and 1750 cm^{-1} are probably the result of the bending motion of the surface water molecules. The strength of the peak of wet NW at about 1600 cm^{-1} is weaker than the one of H_2O, which is probably due to the fact that the number of H_2O molecules is decreased and that the bending motion of the surface water molecules are restricted in the wet NW. The weak peaks between 2000 and 3000 cm^{-1} correspond to the hydrogen bonds between the H_2O molecules and the O of NW. The modes around ~3500 cm^{-1} originate from the stretching modes of O–H bond. Adsorbed surface water contributes bending and stretching modes with frequencies above 1000 cm^{-1}, which provide an additional channel of energy dissipation, compared to vacuum environment. Understanding of resonance frequency matching between electronic transitions and reported normal mode frequencies $\varepsilon_i - \varepsilon_j \approx \hbar\omega_{vib}$ is critical for analyzing of electronic energy dissipation.

The absolute value of the electronic band gap has little effects on the rates of intra-band nonradiative transitions. The PBE and HSE results are similar, so that only the PBE and corrected PBE results are subject of the following discussion.

Interaction of electronic excitations with normal modes (phonons) is a key mechanism for dynamical formation of charge transfer states. An on-the-fly non-adiabatic coupling is a measure of such interaction, and is often computed along ambient temperature molecular dynamics trajectory, as illustrated in Fig. S11. Upon average over ensemble, the influence of phonons onto electrons is dominated by the second order term in the time-dependent perturbation theory, represented by the autocorrelation functions of non-adiabatic coupling. A time average of the autocorrelation functions (Eq. S3a) of the electron-phonon couplings (Eq. S2) provides coefficients of electronic transitions that enter into the equation of motion for the electronic degrees of freedom (Eq. S1a).

The computed autocorrelation function of electron-phonon interaction for the transition from the lowest unoccupied orbital (LU) to the highest occupied orbital (HO) denoted as (HO, LU) is vanishing. Autocorrelation functions for the transitions (LU + 1, LU + 2), (HO − 1, HO), and (LU, LU + 1) decay abruptly as function of time within a few femtoseconds (Fig. S12a). Such abrupt decay witnesses an absence of memory effects, justifies Redfield methodology, and allows to compute the rates of phonon-induced electronic transitions R_{iijj} between pairs of electronic states i and j [38–49]. The curve in Fig. 2(a) summarizes the dependence of such relaxation rates on increase of energy subgap $R_{iijj} = R(\Delta\varepsilon_{ij}), \Delta\varepsilon_{ij} = \varepsilon_i - \varepsilon_j$. Most of numerical data agree with the following trend: $\log_{10}(R_{iijj}/1fs^{-1}) = A + Be^{-\beta\Delta\varepsilon_{ij}}$, with A = −4.93, B = 3.17, and $\beta = 5.45\ eV^{-1}$. In the limit of vanishing subgaps $\Delta\varepsilon_{ij} \to 0$, $e^{-\beta\Delta\varepsilon_{ij}} \approx 1 - \beta\Delta\varepsilon_{ij}$ and the above Equation reads: $\lim_{\Delta\varepsilon_{ij}\to 0}(R_{iijj}) \approx Ce^{-\alpha|\varepsilon_i-\varepsilon_j|}$, with $C = 0.017\ fs^{-1}$ and $\alpha = 39.7\ eV^{-1}$. These fitting constants summarize *ab initio* treatment of phonon-induced electronic transitions and can be used for exploring kinetics of excited electrons and holes. The above fitting agrees with phenomenological "energy-gap law" which is generally applicable to non-radiative processes for a variety of excited states in a broad class of systems [82]. The non-radiative decay constants increase as the emission energies shift to the lower values. The maximal absolute values of the representative Redfield tensor element R_{iijj} (Fig. S12b) appear at i = 3 (HO-3), j = 4 (HO-2) or i = 4, j = 3, and equals to $0.014\ fs^{-1}$. The elements of Redfield tensor connecting states near the band-gap are vanishing.

Next we focus on the carrier non-adiabatic relaxation rates and pathways, and evaluate carrier dynamics at the semiconductor-water interface. For each initial excitation, the average relaxation rates K_e, K_h are computed. Note that such rates include contributions of multiple individual Redfield relaxation rates R_{iijj}. The hole generated in the transition of the highest oscillator strength, loses energy by coupling to phonons and relaxes to the edge of the valence bands within 330 fs (Table S2) for wet NW. The hole excited lower in the valence band takes longer to relax to the HO. The hole relaxes faster in energy than the electron due to different spacing of orbital energies in valence bands and conduction bands. That affects resonance with normal mode frequencies $\Delta\varepsilon_{ij} \approx \hbar\omega_{vib}$.

Fig. 2(b) visualizes typical non-adiabatic relaxation dynamics starting from a transition with the highest oscillator strength. The hole relaxes from HO-15 to HO. The HO-15 orbital is distributed in the O-2p states of the entire nanowire with a small mixing of O states of several water molecules, and the HO orbital is localized on one side of the O-2p states on (1 0 0) surface (see Fig. S13). The hole non-radiative relaxation to the top of valence band results in the localization of hole on the surface of the NW. Spatial dynamics of photoinduced charge carriers is illustrated in Fig. S14. Localization of photo-excited holes prevents fast electron and hole recombination. Upon photo-excitation the hole migrates

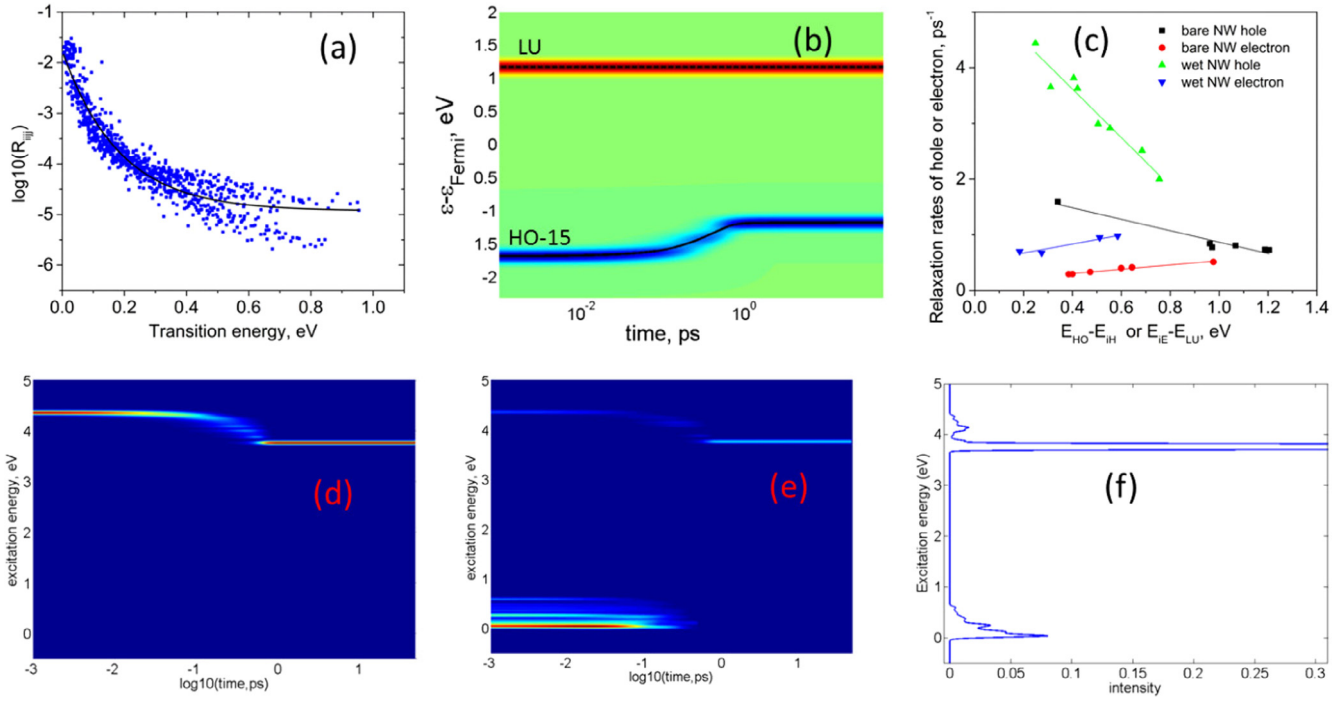

Fig. 2. (a) Probability of non-radiative transitions induced by lattice vibrations vs. intra-band transition energy. The unit of R_{iijj} is fs^{-1}. (b) Non-adiabatic relaxation dynamics for the initial condition corresponding to populating pair of orbitals, which provide transition with the highest oscillator strength. Here, red, green, and blue colored areas label the distribution for gain, no change, and loss, respectively, in comparison with the equilibrium distribution; red areas can be understood as relating to electrons, and blue ones to holes. (c) Relaxation rates of electron K_e and hole K_h for bare and wet TiO_2 NWs. X axis shows the value of the difference of initial and final energies E_{HO}-E_{iH} for hole and E_{iE}-E_{LU} for electron. (d) Simulated photo-excitation dynamics, (e) emission dynamics, and (f) integrated emission spectra of wet TiO_2 NW after photo-excitation at 4.36 eV, corresponding to the transition from HO-15 to LU. Colors correspond to the intensity (oscillator strength) of transition scaled accordingly to the rainbow order: red stays for maximum intensity and navy blue for zero. (For interpretation of the references to color in this figure legend, the reader is referred to the web version of this article.)

to the TiO_2/H_2O interface, and the surface becomes positively charged due to much faster relaxation of hole compared to electron dynamics. Most of femtosecond spectroscopy focuses on monitoring of photoinduced charge transfer dynamics in dye-sensitized TiO_2 compounds. However, Tamaki et al. [83] analyze and compare experimental data on electron and hole migration to the TiO_2 surface concluding that the hole trapping is expected to occur within 50–200 fs range, quicker than electron trapping. Yang and Tamai reported a trapping time of 50 fs for colloidal TiO_2 particles in solution [84]. These observations qualitatively agree with our computation of hole relaxation being quicker than electron relaxation.

Comparison of the calculated relaxation rates of electron and hole for the bare and H_2O adsorbed TiO_2 NW is shown in Fig. 2 (c). Electron and hole relaxation rates have different values and different dependence on energy. For both NWs, the hole dissipates energy faster than the electron $K_e < K_h$, since DOS at the top of the VB is higher than DOS at the bottom of the CB. For both NWs, the electron excited at higher energy up in the conduction band takes shorter time to relax to the LU, as summarized by positive values of rate sensitivity to excitation energy $dK_e^{(bare)}/dE = 0.38\ ps^{-1}\ eV^{-1}$ and $dK_e^{(H2O)}/dE = 0.81\ ps^{-1}\ eV^{-1}$, since at higher excitation energies there are more configurations for matching the electron-phonon resonance condition. At higher excitation energies, the photo-excitation and electron relaxation in reduced wet TiO_2 can be perturbed by additional "wet electron" pathway [85], although in the explored range of excitations we did not observe these signatures.

For both NWs, the hole excited at low energy deep in the valence band takes longer time to relax to the HO, as summarized by negative values of rate's sensitivity to excitation energy $dK_h^{(bare)}/dE = -1.03\ ps^{-1}\ eV^{-1}$ and $dK_h^{(H2O)}/dE = -4.35\ ps^{-1}\ eV^{-1}$, since at higher excitation energies, holes experience larger number of subsequent elementary relaxation steps. The H_2O adsorption on the surface of TiO_2 NW greatly enhances the relaxation rates of holes $K_h^{(H2O)}/K_h^{(bare)} = 4.4$, which may be due to (i) an additional coupling between the electronic states in surface of TiO_2 NW and vibrational modes contributed by H_2O and (ii) better matching the resonance condition for such transitions $\varepsilon_i - \varepsilon_j \approx \hbar\omega_{vib}$. Similar trend is observed for electrons, $K_e^{(H2O)}/K_e^{(bare)} = 2.1$. In wet NWs, computed relaxation of electrons (holes) is approximately 2 (4) times faster when compared with the bare NW. For the wet NW, the calculated non-radiative recombination rate is $5.73 \times 10^{-3}\ ps^{-1}$ (i.e. the respective lifetime is 174.5 ps). For the bare NW, the non-radiative recombination rate is $1.17 \times 10^{-3}\ ps^{-1}$ (i.e. the respective lifetime is 854.7 ps). After intra-band relaxation, the NW remains in the charge transfer excited state for another few hundred picoseconds. We expect that the experimental lifetime should be slightly longer due to the underestimated band gap by PBE. Our results (Fig. S15) show that the radiative recombination lifetimes for both NWs are longer than non-radiative ones, and radiative recombination lifetime of wet NW is also shorter than that of bare NW.

The simulated photo-excitation dynamics, emission dynamics, and integrated emission spectra of wet TiO_2 NW after photo-excitation at 4.36 eV are shown in Fig. 2(d)–(f). Fig. 2(d) shows that the excitation, corresponding to the parent inter-band absorption from HO-15 to LU, has a non-radiative lifetime of 0.2 ps at HO-15 orbital. After that time the hole relaxation induced by the lattice vibrations occurs between 0.2 and 0.6 ps, and remains at the edge of the band gap for longer than 10 ps. The emission dynamics in Fig. 2(e) shows that an emission signal at ~4.4 eV disappears within 0.1 ps and another emission signal at the band edge (~3.7 eV) appears at 0.5 ps [86]. Fig. 2(f) reiterates that besides the strong signal at 4.4 eV, another emission line at ~3.7 eV appears due to band edge luminescence. This is in agreement with the emission dynamics results and PL spectra of anatase TiO_2 particles [87]. There are additional intra-band emission features at IR-range energies less than 1.0 eV, corresponding to the radiative intra-band transitions from CB to CB or from VB to VB for the photo-excited electron or hole. These radiatively allowed transitions with the energies smaller than the band gap can be observed in ultrafast time-resolved pump−probe spectroscopies.

In summary, electronic and optical properties of wet [0 0 1] anatase TiO_2 NRs and NWs have been characterized by UV–vis spectroscopy, *ab initio* electronic structure calculations, density matrix formalism, and non-adiabatic excited state dynamics. The results evaluate potential of this class of materials for photo-catalytic application and for photo-electro-chemical water splitting. Quantum confinement and dangling bond compensation determine the following trend in the calculated band gap values: E_g (wet NW) > E_g (bare NW) > E_g (bulk). Density of occupied states near the valence band maximum is found to be higher than the density of unoccupied states near the conduction band minimum, which is caused by the crystal field splitting of d orbitals into t_{2g} and e_g in the conduction bands. Experimental UV–vis absorption spectrum is compared to and interpreted by use of the calculated absorption spectrum. It reveals features attributed to quantization in transverse direction. The water molecules are partially dissociated at the surface of NW, and more water molecules are dissociated during the MD at 300 K. Significant charge rearrangements occur in the spatial regions between dissociated water and the surface of NW. The adsorbed water provides additional channels of energy dissipation, which enhance the relaxation rates of charge carriers. The non-radiative decay behavior of photoexcitations obtained by *ab initio* treatment of phonon-induced electronic transitions is found consistent with phenomenological "band-gap law". Photoinduced charge carrier dynamics beyond the Born-Oppenheimer approximation using on-the-fly couplings demonstrate possibility of long-lived surface charge transfer excitations. Such charge transfer states are formed with different rates for the wet TiO_2 NWs compared with that for the bare NWs. Specifically, computed relaxation of electrons (holes) is several times faster in wet NWs, than in the bare NW surrounded by vacuum. Several trends support appearance of photoinduced surface charge transfer: (i) holes relax faster than electrons consistent with denser states near the valence band maximum, and (ii) in the lowest excitation, electron density is distributed homogeneously on all Ti ions while hole density tends to localize on surface oxygens. Observations (i) and (ii) prove the formation of long-lived excited state with a positive charge transferred to the surface of nanowire. TiO_2 surface in such states can function as an anode. Positive surface charge is expected to facilitate oxidation of adsorbed molecules. This setup is specially promising for oxidizing water and generating oxygen according to the half reaction: $2H_2O \rightarrow 4H^+ + 4e^- + O_2$.

Acknowledgment

This research was supported by National Science Foundation of the United States (CHE-1413614, ACI-1440681, CHE-0840507, CHE-0722632, EPS-0903804, EPS-0554609), and United States Department of Energy (DOE) (DE-FG02-08ER64624 and DE-EE0000270) BES – Chemical Sciences, NERSC Contract No. DE-AC02-05CH11231, allocation Awards 86898, and 89959 "*Computational Modeling of Photo-catalysis and Photoinduced Charge Transfer Dynamics on Surfaces*", and computational resources of USD High Performance Computing facilities operated by Douglas Jennewein. SPH and DSK thank Peter Deak for discussions on problematic of TiO_2 NWs. DK thanks Talgat Inerbaev, Oleg Prezhdo, David Micha, for inspiring discussions on nonadiabatic dynamics. We also acknowledge support of Center for Integrated Nanotechnology (CINT) and Center for Nonlinear Studies (CNLS) at Los Alamos

National Laboratory (LANL). LANL is operated by Los Alamos National Security, LLC, for the National Nuclear Security Administration of the US Department of Energy under contract DE-AC52-06NA25396. S.K. acknowledges financial support of the U.S. Department of Energy (DOE) Early Career Research grant DE-SC008446.

Appendix A. Supplementary data

Supplementary data associated with this article can be found, in the online version, at http://dx.doi.org/10.1016/j.chemphys.2016.08.002.

References

[1] J. Tang, J.R. Durrant, D.R. Klug, Mechanism of photocatalytic water splitting in TiO_2. Reaction of water with photoholes, importance of charge carrier dynamics, and evidence for four-hole chemistry, J. Am. Chem. Soc. 130 (42) (2008) 13885.
[2] J.B. Joo, R. Dillon, I. Lee, Y.D. Yin, C.J. Bardeen, F. Zaera, Promotion of atomic hydrogen recombination as an alternative to electron trapping for the role of metals in the photocatalytic production of H-2, Proc. Natl. Acad. Sci. USA 111 (22) (2014) 7942.
[3] L.A. King, M.E. Kern, B.A. Parkinson, Sensitization of single crystal substrates, in: D. Kilin (Ed.), Photoinduced Processes at Surfaces and in Nanomaterials, vol. 1196, Amer Chemical Soc., Washington, 2015, pp. 1–45.
[4] A. Fujishima, K. Honda, Electrochemical Photolisis of Water at a Semiconductor Electrode, Nature 238 (5358) (1972) 37.
[5] A. Verdaguer, G.M. Sacha, H. Bluhm, M. Salmeron, Molecular structure of water at interfaces: wetting at the nanometer scale, Chem. Rev. 106 (4) (2006) 1478.
[6] Y. Ping, Y. Li, F. Gygi, G. Galli, Tungsten oxide clathrates for water oxidation: a first principles study, Chem. Mater. 24 (21) (2012) 4252.
[7] A.V. Akimov, A.J. Neukirch, O.V. Prezhdo, Theoretical insights into photoinduced charge transfer and catalysis at oxide interfaces, Chem. Rev. 113 (6) (2013) 4496.
[8] G.S. Li, L.P. Li, J. Boerio-Goates, B.F. Woodfield, High purity anatase TiO_2 nanocrystals: near room-temperature synthesis, grain growth kinetics, and surface hydration chemistry, J. Am. Chem. Soc. 127 (24) (2005) 8659.
[9] H.Z. Zhang, J.F. Banfield, Structural characteristics and mechanical and thermodynamic properties of nanocrystalline TiO_2, Chem. Rev. 114 (19) (2014) 9613.
[10] L. Sang, Y. Zhao, C. Burda, TiO_2 nanoparticles as functional building blocks, Chem. Rev. 114 (19) (2014) 9283.
[11] A.S. Barnard, L.A. Curtiss, Prediction of TiO_2 nanoparticle phase and shape transitions controlled by surface chemistry, Nano Lett. 5 (7) (2005) 1261.
[12] U. Diebold, The surface science of titanium dioxide, Surf. Sci. Rep. 48 (5–8) (2003) 53.
[13] F. De Angelis, C. Di Valentin, S. Fantacci, A. Vittadini, A. Selloni, Theoretical studies on anatase and less common TiO_2 phases: bulk, surfaces, and nanomaterials, Chem. Rev. 114 (19) (2014) 9708.
[14] C. Lee, C.M. Aikens, Water adsorption and dissociation processes on small Mn-doped TiO_2 complexes, J. Phys. Chem. A 118 (3) (2014) 598.
[15] C. Lee, C.M. Aikens, Theoretical investigation of water oxidation processes on small $MnxTi_{2-x}O_4$ (x = 0–2) complexes, J. Phys. Chem. A (2014).
[16] D.J. Vogel, D. Kilin, Electron dynamics of solvated titanium hydroxide, Mol. Phys. 113 (3–4) (2015) 397.
[17] W. Sapp, R. Koodali, D. Kilin, Charge transfer mechanism in titanium-doped microporous silica for photocatalytic water-splitting applications, Catalysts 6 (3) (2016) 12.
[18] A. Vittadini, A. Selloni, F.P. Rotzinger, M. Gratzel, Structure and energetics of water adsorbed at TiO_2 anatase (1 0 1) and (0 0 1) surfaces, Phys. Rev. Lett. 81 (14) (1998) 2954.
[19] Y.B. He, A. Tilocca, O. Dulub, A. Selloni, U. Diebold, Local ordering and electronic signatures of submonolayer water on anatase TiO_2(1 0 1), Nat. Mater. 8 (7) (2009) 585.
[20] G.S. Herman, Z. Dohnalek, N. Ruzycki, U. Diebold, Experimental investigation of the interaction of water and methanol with anatase-TiO_2(1 0 1), J. Phys. Chem. B 107 (12) (2003) 2788.
[21] L.E. Walle, A. Borg, E.M.J. Johansson, S. Plogmaker, H. Rensmo, P. Uvdal, A. Sandell, Mixed dissociative and molecular water adsorption on anatase TiO_2(1 0 1), J. Phys. Chem. C 115 (19) (2011) 9545.
[22] M. Raju, S.Y. Kim, A.C.T. van Duin, K.A. Fichthorn, ReaxFF reactive force field study of the dissociation of water on titania surfaces, J. Phys. Chem. C 117 (20) (2013) 10558.
[23] W.U. Huynh, J.J. Dittmer, A.P. Alivisatos, Hybrid nanorod-polymer solar cells, Science 295 (5564) (2002) 2425.
[24] P. Yang, R. Yan, M. Fardy, Semiconductor nanowire: What's next?, Nano Lett 10 (5) (2010) 1529.
[25] C. Balasanthiran, J.D. Hoefelmeyer, Facile method to attach transition metal ions to the surface of anatase TiO_2 nanorods, Chem. Commun. 50 (43) (2014) 5721.
[26] W. Kang, C.S. Spanjers, R.M. Rioux, J.D. Hoefelmeyer, Synthesis of brookite TiO_2 nanorods with isolated Co(II) surface sites and photocatalytic degradation of 5,8-dihydroxy-1,4-naphthoquinone dye, J. Mater. Chem. A 1 (26) (2013) 7717.
[27] S.T. Pillai, T. Fischer, T.T. Clikeman, J. Esbenshade, C. Berdanier, H. Rohwer, M. Jastram, W. Kang, C. Balasanthiran, C.S. Spanjers, T. Inerbaev, D.S. Kilin, R.M. Rioux, J.D. Hoefelmeyer, Single site metal ions on the surface of TiO_2 nanorods – a platform for theoretical and experimental investigation, Chapter 4, in: ACS Book, Photoinduced Processes at Surfaces and in Nanomaterials, Washington, DC, 2015.
[28] X. Feng, K. Shankar, O.K. Varghese, M. Paulose, T.J. Latempa, C.A. Grimes, Vertically aligned single crystal TiO_2 nanowire arrays grown directly on transparent conducting oxide coated glass: synthesis details and applications, Nano Lett. 8 (11) (2008) 3781.
[29] A. Iacomino, G. Cantele, F. Trani, D. Ninno, DFT Study on anatase TiO_2 nanowires: structure and electronic properties as functions of size, surface termination, and morphology, J. Phys. Chem. C 114 (29) (2010) 12389.
[30] X.D. Wang, Z.D. Li, J. Shi, Y.H. Yu, One-dimensional titanium dioxide nanomaterials: nanowires, nanorods, and nanobelts, Chem. Rev. 114 (19) (2014) 9346.
[31] S.P. Webb, T. Iordanov, S. Hammes-Schiffer, Multiconfigurational nuclear-electronic orbital approach: incorporation of nuclear quantum effects in electronic structure calculations, J. Chem. Phys. 117 (9) (2002) 4106.
[32] M.D. Hack, A.M. Wensmann, D.G. Truhlar, M. Ben-Nun, T.J. Martinez, Comparison of full multiple spawning, trajectory surface hopping, and converged quantum mechanics for electronically nonadiabatic dynamics, J. Chem. Phys. 115 (3) (2001) 1172.
[33] A.W. Jasper, S. Nangia, C.Y. Zhu, D.G. Truhlar, Non-Born-Oppenheimer molecular dynamics, Acc. Chem. Res. 39 (2) (2006) 101.
[34] C.Y. Zhu, A.W. Jasper, D.G. Truhlar, Non-born-oppenheimer Liouville-von Neumann dynamics. Evolution of a subsystem controlled by linear and population-driven decay of mixing with decoherent and coherent switching, J. Chem. Theory Comput. 1 (4) (2005) 527.
[35] J.C. Tully, Molecular dynamics with electronic transitions, J. Chem. Phys. 93 (2) (1990) 1061.
[36] J.C. Tully, Perspective: nonadiabatic dynamics theory, J. Chem. Phys. 137 (22) (2012).
[37] S.V. Kilina, C.F. Craig, D.S. Kilin, O.V. Prezhdo, Ab Initio time-domain study of phonon-assisted relaxation of charge carriers in a PbSe quantum dot, J. Phys. Chem. C 111 (12) (2007) 4871.
[38] S. Fernandez-Alberti, V.D. Kleiman, S. Tretiak, A.E. Roitberg, Nonadiabatic molecular dynamics simulations of the energy transfer between building blocks in a phenylene ethynylene dendrimer, J. Phys. Chem. A 113 (26) (2009) 7535.
[39] T. Nelson, S. Fernandez-Alberti, A.E. Roitberg, S. Tretiak, Nonadiabatic excited-state molecular dynamics: modeling photophysics in organic conjugated materials, Acc. Chem. Res. 47 (4) (2014) 1155.
[40] L.G.C. Rego, V.S. Batista, Quantum dynamics simulations of interfacial electron transfer in sensitized TiO_2 semiconductors, J. Am. Chem. Soc. 125 (26) (2003) 7989.
[41] E. Jakubikova, R.C. Snoeberger, V.S. Batista, R.L. Martin, E.R. Batista, Interfacial electron transfer in TiO(2) surfaces sensitized with Ru(II)-polypyridine complexes, J. Phys. Chem. A 113 (45) (2009) 12532.
[42] D.G. Tempel, A. Aspuru-Guzik, Relaxation and dephasing in open quantum systems time-dependent density functional theory: properties of exact functionals from an exactly-solvable model system, Chem. Phys. 391 (1) (2011) 130.
[43] J.A. Parkhill, D.G. Tempel, A. Aspuru-Guzik, Exciton coherence lifetimes from electronic structure, J. Chem. Phys. 136 (10) (2012) 104510.
[44] E. Tapavicza, G.D. Bellchambers, J.C. Vincent, F. Furche, Ab initio non-adiabatic molecular dynamics, PCCP 15 (42) (2013) 18336.
[45] A.G. Redfield, On the theory of relaxation processes, IBM J. Res. Dev. 1 (1) (1957) 19.
[46] D. Egorova, M. Thoss, W. Domcke, H.B. Wang, Modeling of ultrafast electron-transfer processes: validity of multilevel Redfield theory, J. Chem. Phys. 119 (5) (2003) 2761.
[47] W.T. Pollard, R.A. Friesner, Solution of the redfield equation for the dissipative quantum dynamics of multilevel systems, J. Chem. Phys. 100 (7) (1994) 5054.
[48] W.T. Pollard, A.K. Felts, R.A. Friesner, The Redfield equation in condensed-phase quantum dynamics, Adv. Chem. Phys. 93 (1996) 77.
[49] J.M. Jean, R.A. Friesner, G.R. Fleming, Application of a multilevel Redfield theory to electron transfer in condensed phases, J. Chem. Phys. 96 (8) (1992) 5827.
[50] V. Sundström, T. Pullerits, R. van Grondelle, Photosynthetic light-harvesting: reconciling dynamics and structure of purple bacterial LH2 reveals function of photosynthetic unit, J. Phys. Chem. B 103 (13) (1999) 2327.
[51] O. Kuhn, V. May, M. Schreiber, Dissipative vibrational dynamics in a curve-crossing system, J. Chem. Phys. 101 (12) (1994) 10404.
[52] W.B. Davis, M.R. Wasielewski, M.A. Ratner, V. Mujica, A. Nitzan, Electron transfer rates in bridged molecular systems: a phenomenological approach to relaxation, J. Phys. Chem. A 101 (35) (1997) 6158.
[53] P.A. Apanasevich, S.Y. Kilin, A.P. Nizovtsev, N.S. Onishchenko, Statistics of dephasing perturbations and relaxational processes in a high-power optic field – application to free induction decay, J. Opt. Soc. Am. B Opt. Phys. 3 (4) (1986) 587.
[54] D.S. Kilin, D.A. Micha, Modeling the photovoltage of doped Si surfaces, J. Phys. Chem. C 115 (3) (2010) 770.

[55] J.C. Chen, A. Schmitz, D.S. Kilin, Computational simulation of the p-n doped silicon quantum dot, Int. J. Quantum Chem. 112 (24) (2012) 3879.
[56] J. Chen, A. Schmitz, T. Inerbaev, Q. Meng, S. Kilina, S. Tretiak, D.S. Kilin, First-principles study of p-n-doped silicon quantum dots: charge transfer, energy dissipation, and time-resolved emission, J. Phys. Chem. Lett. 4 (17) (2013) 2906.
[57] T. Vazhappilly, D.S. Kilin, D.A. Micha, Modeling the surface photovoltage of silicon slabs with varying thickness, J. Phys. Condens. Matter 27 (13) (2015) 134204.
[58] T.M. Inerbaev, J.D. Hoefelmeyer, D.S. Kilin, Photoinduced charge transfer from titania to surface doping site, J. Phys. Chem. C 117 (19) (2013) 9673.
[59] S.J. Jensen, T.M. Inerbaev, D.S. Kilin, Spin unrestricted excited state relaxation study of vanadium(IV)-doped anatase, J. Phys. Chem. C 120 (11) (2016) 5890.
[60] Y. Zhang, C. Qiu, D.S. Kilin, Electron dynamics in charged wet TiO_2 anatase (0 0 1) surface functionalised by ruthenium ions, Mol. Phys. 112 (3–4) (2014) 441.
[61] S. Huang, T.M. Inerbaev, D. Kilin, Excited state dynamics of Ru10 cluster interfacing anatase TiO_2(1 0 1) Surface and liquid water, J. Phys. Chem. Lett. 5 (16) (2014) 2823.
[62] S. Kilina, D. Kilin, S. Tretiak, Light-driven and phonon-assisted dynamics in organic and semiconductor nanostructures, Chem. Rev. 115 (12) (2015) 5929–5978.
[63] O.V. Prezhdo, W.R. Duncan, V.V. Prezhdo, Photoinduced electron dynamics at the chromophore-semiconductor interface: a time-domain ab initio perspective, Prog. Surf. Sci. 84 (1–2) (2009) 30.
[64] W.R. Duncan, O.V. Prezhdo, Theoretical studies of photoinduced electron transfer in dye-sensitized TiO_2, Annu. Rev. Phys. Chem. 58 (2007) 143.
[65] S.A. Fischer, W.R. Duncan, O.V. Prezhdo, Ab initio nonadiabatic molecular dynamics of wet-electrons on the TiO_2 surface, J. Am. Chem. Soc. 131 (42) (2009) 15483.
[66] R. Long, N.J. English, O.V. Prezhdo, Photo-induced charge separation across the graphene-TiO_2 interface is faster than energy losses: a time-domain ab lnitio analysis, J. Am. Chem. Soc. 134 (34) (2012) 14238.
[67] R. Long, O.V. Prezhdo, Ab initio nonadiabatic molecular dynamics of the ultrafast electron injection from a Pbse quantum dot into the TiO_2 surface, J. Am. Chem. Soc. 133 (47) (2011) 19240.
[68] R. Long, O.V. Prezhdo, Dopants control electron-hole recombination at perovskite-TiO_2 interfaces: ab initio time-domain study, ACS Nano 9 (11) (2015) 11143.
[69] C.F. Craig, W.R. Duncan, O.V. Prezhdo, Trajectory surface hopping in the time-dependent Kohn-Sham approach for electron-nuclear dynamics, Phys. Rev. Lett. 95 (16) (2005) 163001.
[70] S.A. Fischer, B.F. Habenicht, A.B. Madrid, W.R. Duncan, O.V. Prezhdo, Regarding the validity of the time-dependent Kohn-Sham approach for electron-nuclear dynamics via trajectory surface hopping, J. Chem. Phys. 134 (2) (2011) 024102.
[71] B.F. Habenicht, O.V. Prezhdo, Nonradiative quenching of fluorescence in a semiconducting carbon nanotube: a time-domain ab initio study, Phys. Rev. Lett. 100 (19) (2008) 4.
[72] H.M. Jaeger, S. Fischer, O.V. Prezhdo, Decoherence-induced surface hopping, J. Chem. Phys. 137 (2012). 22A545-8.
[73] S. Meng, J. Ren, E. Kaxiras, Natural dyes adsorbed on TiO_2 nanowire for photovoltaic applications: enhanced light absorption and ultrafast electron injection, Nano Lett. 8 (10) (2008) 3266.
[74] S. Meng, E. Kaxiras, Electron and hole dynamics in dye-sensitized solar cells: influencing factors and systematic trends, Nano Lett. 10 (4) (2010) 1238.
[75] K. Rashwan, G. Sereda, D. Kilin, Adsorption patterns of caffeic acid on titania: affinity, charge transfer and sunscreen applications, Mol. Phys. 114 (3–4) (2016) 498.
[76] S. Huang, D. Kilin, Molecular dynamics of wet TiO_2 NW at T = 300 K. <https://youtu.be/IGVygW_KKEo> (accessed 6/18/2016).
[77] S. Huang, D.S. Kilin, Electronic structure and hot carrier relaxation in ⟨0 0 1⟩ anatase TiO_2 nanowire, Mol. Phys. 112 (3–4) (2014) 539.
[78] H. Ünal, O. Gülseren, Ş. Ellialtıoğlu, E. Mete, Electronic structures and optical spectra of thin anatase nanowires through hybrid density functional and quasiparticle calculations, Phys. Rev. B 89 (20) (2014) 205127.
[79] P. Deák, B. Aradi, A. Gagliardi, H.A. Huy, G. Penazzi, B. Yan, T. Wehling, T. Frauenheim, Possibility of a field effect transistor based on dirac particles in semiconducting anatase-TiO_2 nanowires, Nano Lett. 13 (3) (2013) 1073.
[80] T.M. Henderson, A.F. Izmaylov, G. Scalmani, G.E. Scuseria, Can short-range hybrids describe long-range-dependent properties?, J Chem. Phys. 131 (4) (2009) 9.
[81] S.K. Kim, R.W. Day, J.F. Cahoon, T.J. Kempa, K.D. Song, H.G. Park, C.M. Lieber, Tuning light absorption in core/shell silicon nanowire photovoltaic devices through morphological design, Nano Lett. 12 (9) (2012) 4971.
[82] R. Englman, J. Jortner, Energy gap law for radiationless transitions in large molecules, Mol. Phys. 18 (2) (1970) 145.
[83] Y. Tamaki, A. Furube, M. Murai, K. Hara, R. Katoh, M. Tachiya, Dynamics of efficient electron-hole separation in TiO_2 nanoparticles revealed by femtosecond transient absorption spectroscopy under the weak-excitation condition, PCCP 9 (12) (2007) 1453.
[84] X. Yang, N. Tamai, How fast is interfacial hole transfer? In situ monitoring of carrier dynamics in anatase TiO_2 nanoparticles by femtosecond laser spectroscopy, PCCP 3 (16) (2001) 3393.
[85] K. Onda, B. Li, J. Zhao, K.D. Jordan, J.L. Yang, H. Petek, Wet electrons at the H_2O/TiO_2(1 1 0) surface, Science 308 (5725) (2005) 1154.
[86] S. Huang, D. Kilin, Probability of spontaneous photoemission of photoexcited wet of TiO_2 NW at T = 300 K. <https://youtu.be/NQflDdsBb54> (accessed 6/18/2016).
[87] N.D. Abazović, M.I. Čomor, M.D. Dramićanin, D.J. Jovanović, S.P. Ahrenkiel, J.M. Nedeljković, Photoluminescence of anatase and rutile TiO_2 particles, J. Phys. Chem. B 110 (50) (2006) 25366.